

## Study of the $^{84}\text{Kr}(^3\text{He}, d)^{85}\text{Rb}$ reaction\*

L. R. Medsker, J. N. Bishop, S. C. Headley, and H. T. Fortune

*Department of Physics, University of Pennsylvania, Philadelphia, Pennsylvania 19174*

(Received 22 August 1974)

The  $^{84}\text{Kr}(^3\text{He}, d)^{85}\text{Rb}$  reaction has been studied at a bombarding energy of 18 MeV. The isotopically enriched  $^{84}\text{Kr}$  target was contained in a gas cell with no entrance window. Excitation energies and angular distributions were obtained for 58 levels below  $E_x = 6.2$  MeV in  $^{85}\text{Rb}$ . A distorted-wave analysis was used to determine  $l$  values and spectroscopic strengths. The results are compared with previous data from transfer reactions and radioactive decay.

$$\left[ \begin{array}{l} \text{NUCLEAR REACTIONS } ^{84}\text{Kr}(^3\text{He}, d), E = 18 \text{ MeV; enriched target; measured} \\ \sigma(E_d, \theta); \text{ deduced } ^{85}\text{Rb} \text{ levels, } l, j, G_{lj}. \end{array} \right]$$

### I. INTRODUCTION

Nuclei with a closed neutron shell at  $N=50$  have been studied<sup>1,2</sup> with transfer reactions and are reasonably well described by the simple shell model. The low-lying proton states<sup>3</sup> are characterized by  $2p_{3/2}$ ,  $1f_{5/2}$ ,  $2p_{1/2}$ , and  $1g_{9/2}$  orbitals, and nuclei in this region are to some extent doubly magic at  $Z=38$  and 40. Holes in the  $N=50$  core, however, create a more complex situation.

The  $^{85}\text{Rb}$  nucleus is interesting because it is in a region of transition away from the  $N=50$  closed shell. Spherical shell-model calculations<sup>4</sup> have had some qualitative success in this region; however, there are indications that nuclei in the  $N \lesssim 50$ ,  $Z \lesssim 40$  region are deformed and that Nilsson model calculations are needed.<sup>5</sup>

The present work is the beginning of a study of the systematics of proton states around  $Z=36$ . A comparison with data from other experiments<sup>1-3, 6-8</sup> on  $^{85}\text{Rb}$  should be helpful in testing the various models.

### II. EXPERIMENTAL PROCEDURE

The experiment was performed with the 18-MeV  $^3\text{He}$  beam from the University of Pennsylvania tandem accelerator. The outgoing deuterons were momentum analyzed with a multiangle spectrograph. Spectra (see Fig. 1) were recorded on Ilford K2 emulsion plates in  $7.5^\circ$  steps starting at  $7.5^\circ$ . The target was enriched  $^{84}\text{Kr}$  gas (90.2%) and was recirculated through a gas cell with no entrance window.<sup>9</sup> The pressure in the gas cell was maintained at 20 Torr, which corresponds to an effective target thickness of  $80 \mu\text{g}/\text{cm}^2$ . The energy resolution was 22 keV full width at half-maximum (FWHM). The gas reservoir contained

a titanium absorber which minimized contamination by carbon, nitrogen, and oxygen. Contamination due to  $^{40}\text{Ar}$  (from the atmosphere) was 2% and a separate run using  $^{40}\text{Ar}$  gas was made in order to identify peaks due to the  $^{40}\text{Ar}(^3\text{He}, d)^{41}\text{K}$  reaction. The other contaminants were  $^{86}\text{Kr}$  (4.6%),  $^{83}\text{Kr}$  (4.9%), and  $^{82}\text{Kr}$  (0.3%), and the states from reactions on these isotopes were identified or were negligibly small. The data were analyzed with the program AUTOFIT<sup>10</sup> in order to obtain excitation energies and cross sections. The measured angular distributions were compared with the results of distorted-wave Born-approximation (DWBA) calculations, using the code DWUCK.<sup>11</sup> The optical model parameters<sup>1</sup> are listed in Table I. The spectroscopic strengths  $G_{lj} = [(2J_f + 1)/(2J_i + 1)] C^2 S_{ij}$  were derived from the differential cross sections by use of the expression

$$\frac{d\sigma}{d\Omega} = 4.42 G_{lj} \sigma_{\text{DWUCK}} / (2j + 1),$$

where  $J_i$ ,  $J_f$ , and  $j$  are the total angular momenta of the target nucleus, residual nucleus, and the transferred proton, respectively.

### III. RESULTS

In the present experiment, 58 levels in  $^{85}\text{Rb}$  were identified up to an excitation energy of 6185 keV. By comparison of calculated DWBA curves and experimental angular distributions, the  $l_p$  values could be determined for most of the states. Figure 2 shows the angular distribution for the ground state (which is the only state observed here to be reached by  $l_p = 3$ ) and those for four states reached by  $l_p = 4$  transfer. Nine states were assigned  $l_p = 1$  (Fig. 3) and 30 states were reached by  $l_p = 2$  transfer (Figs. 4 and 5). Eleven states

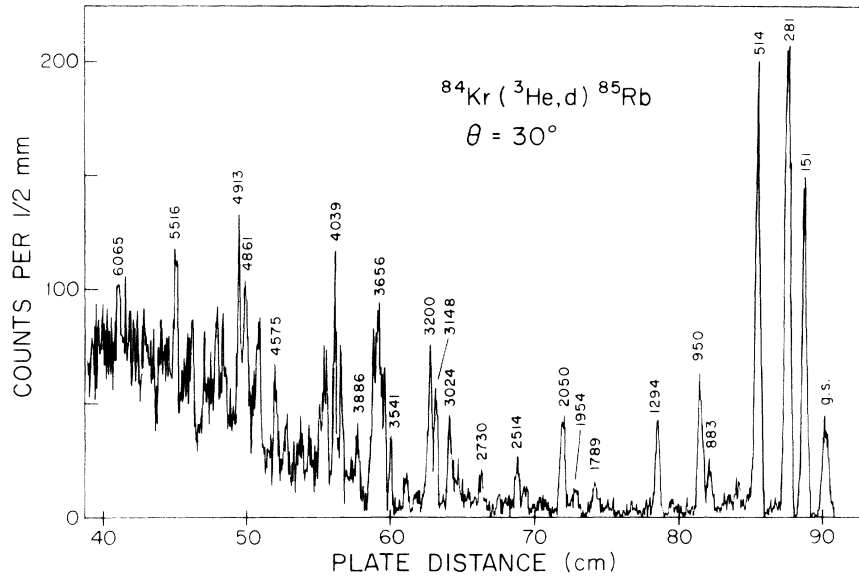


FIG. 1. Typical deuteron spectrum of the  $^{84}\text{Kr}({}^3\text{He}, d){}^{85}\text{Rb}$  reaction.

had angular distributions characteristic of  $l_p = 0$  (Fig. 6). Listed in Table II are the energies of the states, along with  $l_p$  values, spins, and spectroscopic strengths.

The spins of the first four states are well established.<sup>2, 3, 8</sup> The present measurements are consistent with previous data, as shown in Table III. The  $\frac{5}{2}^-$  ground state and  $\frac{3}{2}^-$  151-keV state are reached by  $l_p = 3$  and 1 transfers, respectively, in  $({}^3\text{He}, d)$ . The  $\frac{1}{2}^-$  and  $\frac{9}{2}^+$  states at 281 and 514 keV are both weak in pickup reactions<sup>2, 6</sup> and are reached by strong  $l_p = 1$  and  $l_p = 4$  transfers in the present stripping experiment. A state at 731.9 keV was assigned  $\frac{3}{2}^-$  from Coulomb excitation.<sup>8</sup> A state at about this energy has been observed in pickup and stripping reactions and the  $l_p = 1$

TABLE I. Optical-model parameters used in distorted-wave Born-approximation calculations of  $^{84}\text{Kr}({}^3\text{He}, d){}^{85}\text{Rb}$ .

	${}^3\text{He}$	$d$	Bound-state proton
$V$ (MeV)	170	98	
$r_0$ (fm)	1.14	1.10	1.20
$a$ (fm)	0.75	0.85	0.65
$W$ (MeV)	20	...	
$W'$ (MeV)	...	72	
$r'_0$ (fm)	1.60	1.40	
$a'$ (fm)	0.80	0.70	
$r_c$ (fm)	1.40	1.30	1.20
$V_{\text{so}}$ (MeV)	...	6.0	$\lambda = 25$

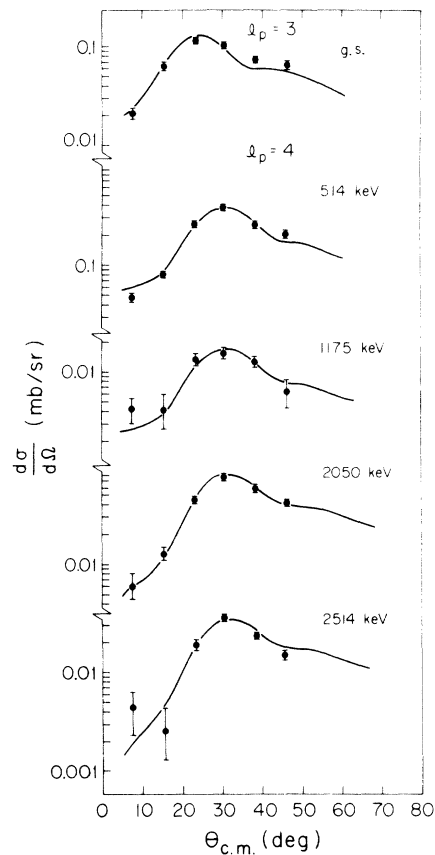


FIG. 2. Angular distributions of the deuterons leading to states in  ${}^{85}\text{Rb}$  from the  ${}^{84}\text{Kr}({}^3\text{He}, d){}^{85}\text{Rb}$  reaction. The solid lines are the distorted-wave Born-approximation calculations for  $l_p = 3$  and  $l_p = 4$  transfers.

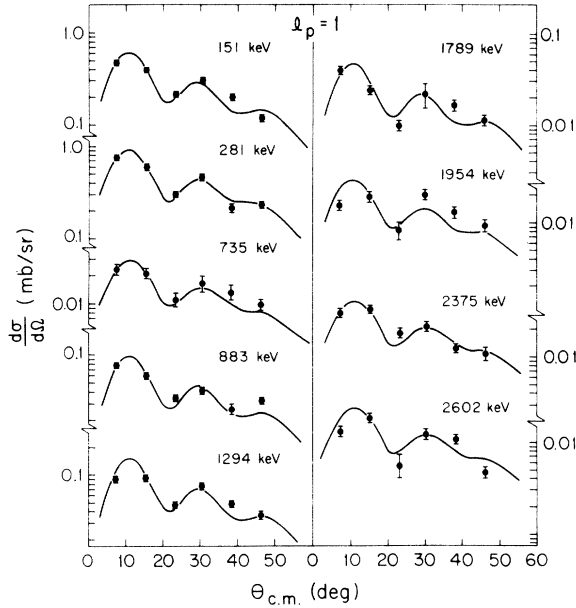


FIG. 3. Angular distributions for levels excited by  $l_p = 1$  transfers in the  $^{84}\text{Kr}(^3\text{He}, d)^{85}\text{Rb}$  reaction. The solid lines are the distorted-wave Born-approximation calculations.

assignment from  $(d, ^3\text{He})$  and  $(^3\text{He}, d)$  is consistent with  $J^\pi = \frac{3}{2}^-$ . A tentative assignment of  $l_p = (3, 4)$  from  $(t, \alpha)$  is in disagreement; however, in that experiment the  $l_p$  assignment is not firm.

A more serious ambiguity in  $^{85}\text{Rb}$  concerns the levels at 868.05 and 880 keV. Vatai *et al.*<sup>12</sup> have given evidence that the level at 868.5 keV has  $J^\pi = (\frac{5}{2}, \frac{7}{2}, \frac{9}{2})^-$ , consistent with a  $J^\pi = \frac{7}{2}^-$  assignment to a level at 868.05 keV from Coulomb excitation.<sup>8</sup> Vatai *et al.* show that the state at 880 keV that was assigned from earlier  $^{85}\text{Sr}$  decay measurements was probably due to contaminating activity. However, recent Coulomb excitation,  $(t, \alpha)$ ,  $(d, ^3\text{He})$ , and the present  $(^3\text{He}, d)$  measurements all show evidence for a state with an energy of about 880 keV and  $J^\pi = (\frac{1}{2}, \frac{3}{2})^-$ . Therefore, even though the 880-keV state was probably not populated in  $^{85}\text{Sr}$  decay, two states appear to exist here—one with  $E_x = 868.05$  keV and  $J^\pi = \frac{7}{2}^-$ , and another with  $E_x = 878.2$  keV and  $J^\pi = \frac{1}{2}^-$  or  $\frac{3}{2}^-$ .

The  $J^\pi$  restrictions for the remaining states in  $^{85}\text{Rb}$  with  $E_x > 900$  keV come from  $(t, \alpha)$ ,  $(d, ^3\text{He})$ , and the present  $(^3\text{He}, d)$  results. A state at  $E_x = 919$  keV was observed<sup>2</sup> in  $(d, ^3\text{He})$  with  $l_p = 3$ . This agrees in energy with a state reported in

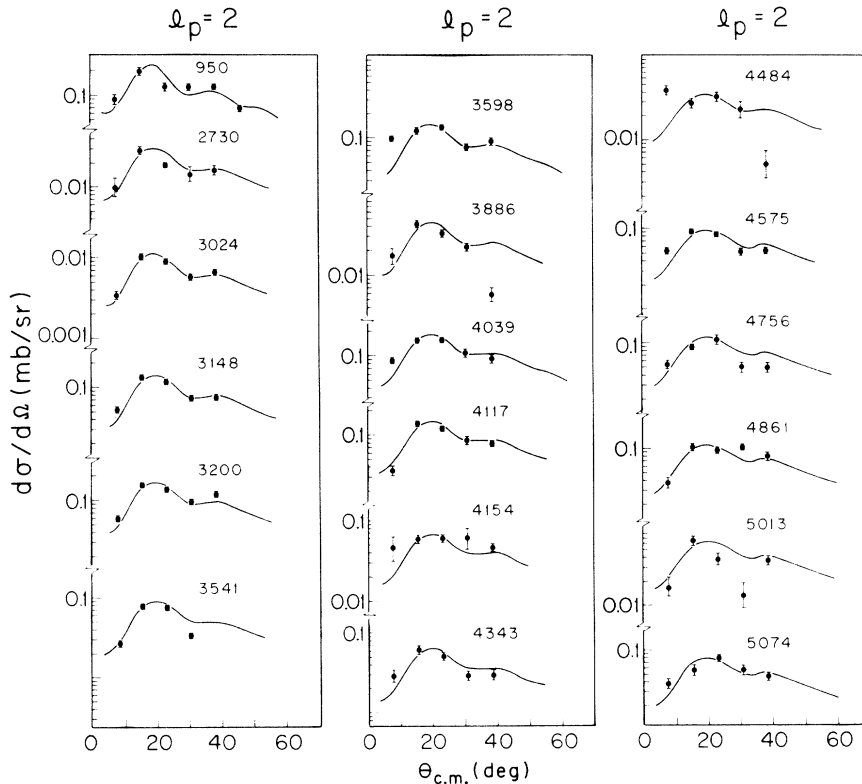


FIG. 4. Angular distributions for levels ( $E_x \leq 5074$  keV) excited by  $l_p = 2$  transfers in the  $^{84}\text{Kr}(^3\text{He}, d)^{85}\text{Rb}$  reaction. The solid lines are the distorted-wave Born-approximation calculations.

TABLE II. Present results for the  $^{84}\text{Kr}(^3\text{He},d)^{85}\text{Rb}$  reaction.

$E_x^a$ (keV)	$l_p$	$J^\pi$	$(2J+1)C^2S$	$E_x^a$ (keV)	$l_p$	$J^\pi$	$(2J+1)C^2S$
0	3	$\frac{5}{2}^-$ b	1.78	3981	0	$\frac{1}{2}^+$	0.046
151	1	$\frac{3}{2}^-$ b	0.82	4039	2	$(\frac{3}{2}, \frac{5}{2})^+$	0.16
281	1	$\frac{1}{2}^-$ c	1.53	4117	2	$(\frac{3}{2}, \frac{5}{2})^+$	0.15
514	4	$\frac{9}{2}^+$ b	6.84	4154	(2)	$(\frac{3}{2}^+, \frac{5}{2}^+)$	0.059
735	1	$(\frac{1}{2}, \frac{3}{2})^-$	0.087	4220	(0)	$(\frac{1}{2}^+)$	0.019
883	(1)	$(\frac{1}{2}^-, \frac{3}{2}^-)$	0.14	4343	2	$(\frac{3}{2}, \frac{5}{2})^+$	0.064
950	2	$(\frac{3}{2}, \frac{5}{2})^+$	0.35	4484	2	$(\frac{3}{2}, \frac{5}{2})^+$	0.029
1175	4	$(\frac{7}{2}, \frac{9}{2})^+$	0.26	4575	2	$(\frac{3}{2}, \frac{5}{2})^+$	0.082
1294	1	$(\frac{1}{2}, \frac{3}{2})^-$	0.18	4631	0	$\frac{1}{2}^+$	0.011
1789	1	$(\frac{1}{2}, \frac{3}{2})^-$	0.046	4729	1	$(\frac{1}{2}, \frac{3}{2})^-$	0.082
1954	1	$(\frac{1}{2}, \frac{3}{2})^-$	0.027	4756	2	$(\frac{3}{2}, \frac{5}{2})^+$	0.089
2050	4	$(\frac{7}{2}, \frac{9}{2})^+$	1.05	4861	2	$(\frac{3}{2}, \frac{5}{2})^+$	0.096
2375	1	$(\frac{1}{2}, \frac{3}{2})^-$	0.039	4913	0	$\frac{1}{2}^+$	0.052
2514	4	$(\frac{7}{2}, \frac{9}{2})^+$	0.46	5013	2	$(\frac{3}{2}, \frac{5}{2})^+$	0.058
2602	1	$(\frac{1}{2}, \frac{3}{2})^-$	0.019	5074	2	$(\frac{3}{2}, \frac{5}{2})^+$	0.050
2730	2	$(\frac{3}{2}, \frac{5}{2})^+$	0.038	5127	2	$(\frac{3}{2}, \frac{5}{2})^+$	0.042
2801	0	$\frac{1}{2}^+$	0.0072	5186	0	$\frac{1}{2}^+$	0.012
2948	0	$\frac{1}{2}^+$	0.015	5245	2	$(\frac{3}{2}, \frac{5}{2})^+$	0.065
3024	2	$(\frac{3}{2}, \frac{5}{2})^+$	0.13	5367	(2)	$(\frac{3}{2}^+, \frac{5}{2}^+)$	0.063
3148	2	$(\frac{3}{2}, \frac{5}{2})^+$	0.16	5444	2	$(\frac{3}{2}, \frac{5}{2})^+$	0.039
3200	2	$(\frac{3}{2}, \frac{5}{2})^+$	0.18	5516	0	$\frac{1}{2}^+$	0.034
3310	(1)	$(\frac{1}{2}^-, \frac{3}{2}^-)$	0.023	5563	(2)	$(\frac{3}{2}^+, \frac{5}{2}^+)$	0.039
3398	1	$(\frac{1}{2}, \frac{3}{2})^-$	0.027	5643	(2)	$(\frac{3}{2}^+, \frac{5}{2}^+)$	0.029
3541	2	$(\frac{3}{2}, \frac{5}{2})^+$	0.089	5668	2	$(\frac{3}{2}, \frac{5}{2})^+$	0.029
3598	2	$(\frac{3}{2}, \frac{5}{2})^+$	0.14	5719	(1)	$(\frac{1}{2}^-, \frac{3}{2}^-)$	0.048
3656 <sup>d</sup>	0	$\frac{1}{2}^+$	0.048	5815	(2)	$(\frac{3}{2}^+, \frac{5}{2}^+)$	0.039
	2	$(\frac{3}{2}, \frac{5}{2})^+$	0.039	5996	(2)	$(\frac{3}{2}^+, \frac{5}{2}^+)$	0.067
3698	0	$\frac{1}{2}^+$	0.10	6065	0	$\frac{1}{2}^+$	0.034
3886	2	$(\frac{3}{2}, \frac{5}{2})^+$	0.047	6185	2	$(\frac{3}{2}, \frac{5}{2})^+$	0.036

<sup>a</sup> Uncertainties are  $\pm 5$  for  $E_x \leq 2730$  and  $\pm 10$  for  $E_x > 2730$ .

<sup>b</sup> See Ref. 3.

<sup>c</sup> See Ref. 8.

<sup>d</sup> Doublet.

Coulomb excitation and in  $(t, \alpha)$ ; however, in the latter, an  $l_p=1$  assignment was made. The 919-keV state was not populated in  $(^3\text{He}, d)$ . We observe strong  $l_p=2$  transfer to a state at 950 keV, consistent in energy with states observed in Coulomb excitation and pickup reactions. The latter, however, report<sup>2,6</sup>  $l_p$  values of 1 and (3, 4). This indicates the existence near 950 keV of a second state that is not populated in  $(^3\text{He}, d)$ .

Definite  $l_p=4$  and  $l_p=1$  transfers are observed in the  $(^3\text{He}, d)$  reaction to states at 1175 and 1294 keV, respectively. The  $l_p$  assignments from pickup reactions for states with similar energies are sufficiently ambiguous that consideration of the existence of more than these two states is not warranted on the basis of available data.

Above  $E_x=1300$  keV, little correlation exists between states observed in pickup and those of

the present ( $^3\text{He}, d$ ) experiment. States at 1384, 1504, and 1639 keV are strong in pickup and might be expected to be weak in ( $^3\text{He}, d$ ). Many new levels in  $^{85}\text{Rb}$  are proposed above  $E_x = 1300$  keV on the basis of the present ( $^3\text{He}, d$ ) data. Table II contains their energies,  $l_p$  values, possible  $J^\pi$  assignments, and spectroscopic strengths.

The summed spectroscopic strengths for the various  $l_p$  values are shown in Table IV. The total for  $l_p = 1, 3$ , and 4 is 13.46. The value expected from the sum rule is 13.85:

$$\sum G_{l_j}(T_<) = [\text{No. proton holes in } N = 50] - \sum G_{l_j}(T_>) \\ = 14 - 2/13 = 13.85.$$

This agreement is excellent, since uncertainties in target thickness and in the DWBA formalism are certainly more than 20%.

One might expect from the simple shell model that  $2p_{3/2}$ ,  $2p_{1/2}$ , and  $1g_{9/2}$  would be the active low-lying proton orbitals above  $Z = 36$  and therefore  $\sum G_{l_j}$  would be nearly 4 for  $l_p = 1$  and 10 for  $l_p = 4$ . For example, in the  $^{88}\text{Sr}(^3\text{He}, d)$  reaction most of the low-lying strength goes to the  $\frac{1}{2}^-$  and  $\frac{9}{2}^+$  states, as depicted in Fig. 7. The  $^{86}\text{Sr}(^3\text{He}, d)$  results,

with  $N = 48$ , show the effects of the two neutron holes—lower excitation energies, greater density of states, and increase in  $l_p = 3$  strength. The present  $^{84}\text{Kr}(^3\text{He}, d)$  results show similar effects including strong  $l_p = 3$  strength ( $\sum G_{l_j} \approx 2$ ). Most of the remaining strength below 2600 keV is fractionated among  $l_p = 1$  and  $l_p = 4$  transfers. The wave function for  $^{84}\text{Kr}$  is thus relatively complicated and contains more vacancies than expected in the  $1f_{5/2}$  and  $2p_{3/2}$  orbitals.

The strength above  $E_x = 2600$  keV is almost entirely  $l_p = 0$  and  $l_p = 2$ . It is fragmented among over 40 states with no single state having  $G_{l_j} > 0.2$ . The sums of  $l_p = 0$  and  $l_p = 2$  strengths observed below 6.2-MeV excitation energy in the present experiment are each about 25% of the strengths expected from the shell model. In Table IV is also shown a comparison of the present spectroscopic strengths with those measured<sup>1, 13</sup> in ( $^3\text{He}, d$ ) reactions on  $^{86}\text{Sr}$  and  $^{88}\text{Sr}$ . The sums of  $l_p = 4$  strengths are quite comparable for all three targets, indicating that the  $1g_{9/2}$  components of the wave functions are about the same. The summed  $l_p = 3$  strengths for  $^{84}\text{Kr}_{48}$  and  $^{86}\text{Sr}_{48}$  are

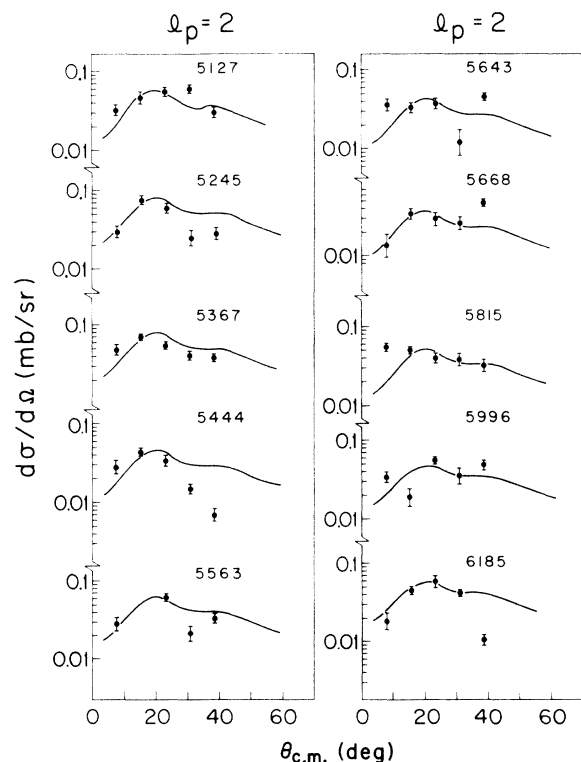


FIG. 5. Angular distributions for levels ( $E_x \geq 5127$ ) excited by  $l_p = 2$  transfers in the  $^{84}\text{Kr}(^3\text{He}, d)^{85}\text{Rb}$  reaction. The solid lines are the distorted-wave Born-approximation calculations.

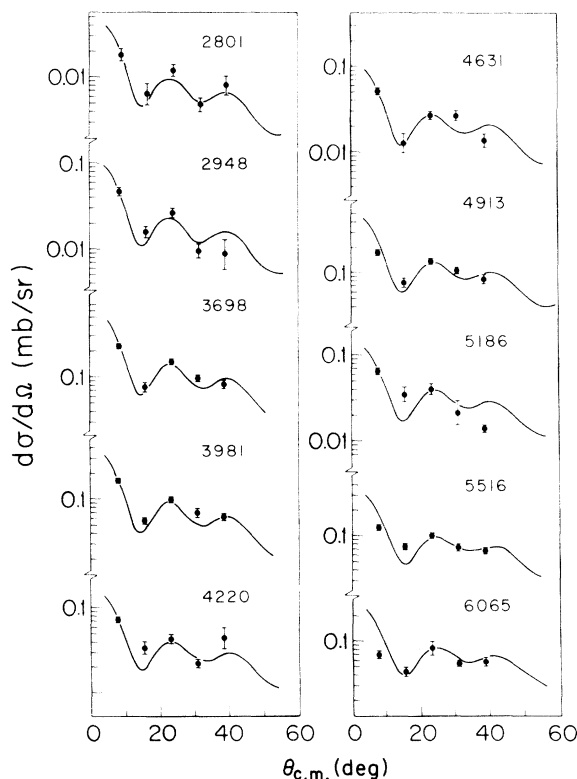


FIG. 6. Angular distributions for levels excited by  $l_p = 0$  transfers in the  $^{84}\text{Kr}(^3\text{He}, d)^{85}\text{Rb}$  reaction. The solid lines are the distorted-wave Born-approximation calculations.

TABLE III. Energy levels,  $l_p$ ,  $J^\pi$ , and spectroscopic strengths for states in  $^{85}\text{Rb}$  from previous experiments compared with the results of the present  $^{84}\text{Kr}(^3\text{He}, d)$  study.

NDS, ( $n, n'\gamma$ ), and Coul. ex.		$^{86}\text{Sr}(t, \alpha)^{85}\text{Rb}$			$^{86}\text{Sr}(d, ^3\text{He})^{85}\text{Rb}$			$^{84}\text{Kr}(^3\text{He}, d)^{85}\text{Rb}$			
$E_x^a$	$J^\pi$	$E_x^a$	$l_p$	$C^2S$	$E_x^b$	$l_p$	$C^2S$	$E_x$	$l_p$	$J^\pi$	$(2J+1)C^2S$
0	$\frac{5}{2}^-$	0	3	3.7	0	3	3.1	0	3	$\frac{5}{2}^-$	1.78
151.18	$\frac{3}{2}^-$	151.5 (0.2)	1	2.1	151	1	2.3	151	1	$\frac{3}{2}^-$	0.82
281.04	$\frac{1}{2}^-$	281 (2)	1	0.5	281	1	0.51	281	1	$\frac{1}{2}^-$	1.53
513.998	$\frac{9}{2}^+$	514 (3)	4	0.7	514	4	0.91	514	4	$\frac{9}{2}^+$	6.84
731.9	$\frac{3}{2}^-$	732 (6)	(3, 4)	0.1	732	1	0.023	735	1	$(\frac{3}{2})^-$	0.087
868.05	$\frac{7}{2}^-$										
878.2		880 (7)	1	0.2	868	1	0.088	883	1	$(\frac{1}{2}, \frac{3}{2})^-$	0.14
919 (1)		925 (10)	1	0.1	919	3	0.28				
951 (1)					951	1	0.062	950	2	$(\frac{5}{2}^+)$	0.35
		960 (10)	(3, 4)	0.2							
1175 (1)		1172 (5)	(3, 4)	0.2	1175 (3)		0.14	1175	4	$(\frac{7}{2}, \frac{9}{2})^+$	0.26
1294 (1)		1291 (7)	1	0.1	1294	3	0.71	1294	1	$(\frac{1}{2}, \frac{3}{2})^-$	0.18
1383 (1)		1375 (8)	(3, 4)		1384	3	0.45				
1445 (1)											
		1492 (8)	1	0.2	1504	1	0.19				
		1627 (4)	3	0.9	1639	3	0.98				
		1792 (15)	(3, 4)	0.08				1789	1	$(\frac{1}{2}, \frac{3}{2})^-$	0.046
		1891 (15)	(3, 4)	(0.10)							
		1940 (10)		(0.07)				1954	1	$(\frac{1}{2}, \frac{3}{2})^-$	0.027
		2006 (10)		(0.10)							
		2056 (5)		(0.20)				2050	4	$(\frac{7}{2}, \frac{9}{2})^+$	1.05
		2191 (10)	(1)	0.12	2212	1	0.14				
		2304 (12)		(0.13)							
								2375	1	$(\frac{1}{2}, \frac{3}{2})^-$	0.039
								2514	4	$(\frac{7}{2}, \frac{9}{2})^+$	0.46
								2602	1	$(\frac{1}{2}, \frac{3}{2})^-$	0.019
								2732	2	$(\frac{3}{2}, \frac{5}{2})^+$	0.038
		4195 (10)	(3)	0.10							

<sup>a</sup> Uncertainties are indicated in keV.

<sup>b</sup> Energy resolution was about 50 keV.

nearly the same though slightly larger for  $^{84}\text{Kr}$ . Most of the difference is for  $l_p = 1$ . The larger  $1f$  strength in  $^{84}\text{Kr}$  compared to that for  $^{88}\text{Sr}$  shows the effect of removing two neutrons.

A comparison of  $l_p = 0$  and  $l_p = 2$  strengths is difficult because of the different ranges of excitation energies covered in the three experiments. The measured  $l_p = 2$  strength does appear to be less for  $^{84}\text{Kr}$  than for  $^{88}\text{Sr}$ , perhaps due to greater fragmentation in the former. On the other hand,

virtually no  $l_p = 0$  strength is reported for  $(^3\text{He}, d)$  on  $^{86}\text{Sr}$  and  $^{88}\text{Sr}$ , whereas the present measurements reveal about  $\frac{1}{4}$  of the sum rule strength for  $l = 0$ .

The distributions of strength for the various  $l_p$  values are shown in Fig. 8. The  $l_p = 0$  and  $l_p = 1$  strengths show normal fragmentation concentrated around excitation energies of 4.340 and 0.685 MeV, respectively. For the  $l_p = 2$  strengths, however, the presence of the additional relatively

			(1/2, 3/2) <sup>-</sup> (0.08, 0.07) 3490
	(5/2) <sup>+</sup>	0.09 3406	
	(5/2) <sup>+</sup>	0.16 3353	
	(5/2) <sup>+</sup>	0.11 3306	
	1/2 <sup>+</sup>	0.04 3195	
	(5/2) <sup>+</sup>	0.25 3090	
	(5/2) <sup>+</sup>	0.20 3043	
	(5/2) <sup>+</sup>	0.11 2995	
	(5/2) <sup>+</sup>	0.12 2907	
	(5/2) <sup>-</sup>	0.16 2730	
(3/2, 5/2) <sup>+</sup>		0.038 2730	
(1/2, 3/2) <sup>-</sup>		0.019 2602	
(7/2, 9/2) <sup>+</sup>		0.46 2514	
(1/2, 3/2) <sup>-</sup>		0.039 2375	
(7/2, 9/2) <sup>+</sup>		1.05 2050	
(1/2, 3/2) <sup>-</sup>		0.027 1954	
(1/2, 3/2) <sup>-</sup>		0.046 1789	
	(5/2) <sup>+</sup>	0.03 2407	
	(5/2) <sup>-</sup>	0.14 2278	
	(9/2) <sup>+</sup>	0.79 2203	
	(1/2, 3/2) <sup>-</sup>	(0.10, 0.09) 2085	
	(1/2, 3/2) <sup>-</sup>	0.07 1848	
	(9/2) <sup>+</sup>	0.53 1605	(5/2) <sup>-</sup> 0.55 1735
			(1/2, 3/2) <sup>-</sup> (0.54, 0.44) 1490
(1/2, 3/2) <sup>-</sup>		0.18 1294	
(7/2, 9/2) <sup>+</sup>		0.26 1175	
	(5/2) <sup>+</sup>	0.32 1155	
	(1/2, 3/2) <sup>-</sup>	(0.60, 0.54) 982	
(5/2) <sup>+</sup>		0.35 950	9/2 <sup>+</sup> 8.8 896
(1/2) <sup>-</sup>		0.14 883	
3/2 <sup>-</sup>		0.087 735	
	(5/2) <sup>-</sup>	1.15 793	
9/2 <sup>+</sup>		6.84 514	
	9/2 <sup>+</sup>	7.19 380	
1/2 <sup>-</sup>		1.53 281	
3/2 <sup>-</sup>		0.82 151	
5/2 <sup>-</sup>		1.78 0	1/2 <sup>-</sup> 1.8 0
$^{84}\text{Kr}(^3\text{He}, d)^{85}\text{Rb}_{48}$	$^{86}\text{Sr}(^3\text{He}, d)^{87}\text{Y}_{48}$		$^{88}\text{Sr}(^3\text{He}, d)^{89}\text{Y}_{50}$
		1.15 0	

FIG. 7. Comparison of energy levels,  $J^\pi$ , and spectroscopic strengths for the  $(^3\text{He}, d)$  reactions on  $^{84}\text{Kr}$  (present)  $^{86}\text{Sr}$  (Ref. 1), and  $^{88}\text{Sr}$  (Ref. 13).

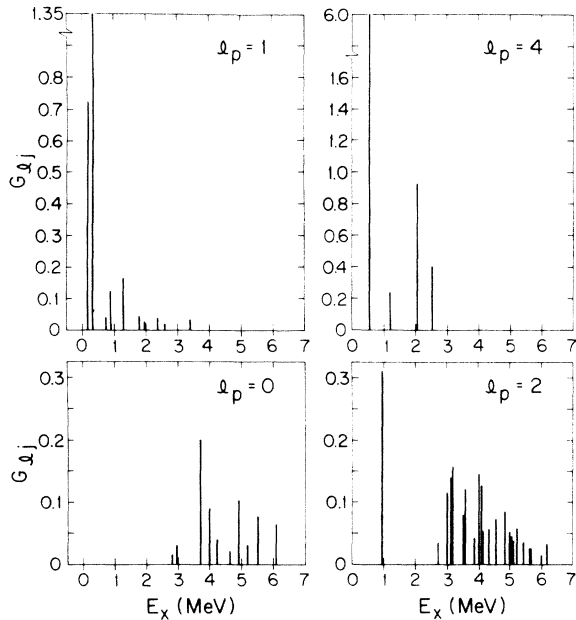


FIG. 8. Distributions of spectroscopic strengths for  $l_p = 0, 1, 2,$  and  $4$  transfers to levels in  $^{85}\text{Rb}$  with the  $^{84}\text{Kr}(^3\text{He}, d)$  reaction.

strong low-lying  $l_p = 2$  state at 950 keV is a notable exception. The high-lying  $l_p = 4$  states at 2050 and 2514 keV are also candidates for anomalous behavior. An interesting possibility is that these three states are  $\frac{5}{2}^+, \frac{7}{2}^+$ , and  $\frac{9}{2}^+$  members of a core-excited high-spin multiplet. No calculations of levels in  $^{85}\text{Rb}$  are available for comparison with the present results; however, Fig. 9 shows a comparison (for even-parity states only) of theoretical and experimental work on  $^{83}\text{Rb}$ . The de-

TABLE IV. Sums of spectroscopic strength for various  $l_p$  transfers in the  $(^3\text{He}, d)$  reactions on  $^{84}\text{Kr}$ ,  $^{86}\text{Sr}$ , and  $^{88}\text{Sr}$ . The region of excitation energy  $E_x$  over which data are available is indicated in the last line.

$l_p$	$^{84}\text{Kr}_{48}$ (Present work)	$^{86}\text{Sr}_{48}$ (Ref. 1)	$^{88}\text{Sr}_{50}$ (Ref. 13)
3	1.78	1.45	0.55
1	3.07	1.86	2.32
4	8.61	8.51	8.80
2	2.45	1.39	4.3
0	0.38	0.04	...
$E_x$ (MeV)	<6.2	<3.5	<5.3

